Quantum-State Controlled Chemical Reactions of Ultracold Potassium-Rubidium Molecules

S. Ospelkaus, *et al.*

Science **327**, 853 (2010);
DOI: 10.1126/science.1184121

peak at 0.5 torr is 0.55, and the overall CO coverage is 0.97. The coverage of CO molecules bound to low-coordinated Pt atoms is defined as the ratio of the number of CO molecules adsorbed at low-coordinated Pt atoms to the number of surface Pt atoms.
29. The ratio of the O1s peak area from CO bound to low-coordinated Pt atoms to the total peak O1s area of CO at 10^{-8} to 10^{-7} torr is 0.35 to 0.40; the overall CO coverage at this pressure is ~0.56.
30. The experimental work was supported by the director, Office of Basic Energy Sciences, Materials Sciences, and Chemical, Geosciences, and Biosciences Divisions. The theoretical work was supported by the Office of Advanced Scientific Computing Research. U.S. Department of Energy under Contract No. DE-AC02-05CH11231. The computation uses the resources of National Energy Research Scientific Computing Center (NERSC) and the INCITE project allocations within the National Center for Computational Sciences (NCCS). XPS data were collected at the Advanced Light Source, Berkeley, CA.
F.T. acknowledges the discussions with S. L. Bernasek, N. Kruse, T. Bligaard, and F. Ogletree.

Supporting Online Material
www.sciencemag.org/cgi/content/full/327/5967/850/DC1
Materials and Methods
SOM Text
Figs. S1 to S13
Tables S1 and S2
References

17 September 2009; accepted 24 December 2009
10.1126/science.1182122

Quantum-State Controlled Chemical Reactions of Ultracold Potassium-Rubidium Molecules

S. Ospelkaus,[1]* K.-K. Ni,[1]* D. Wang,[1] M. H. G. de Miranda,[1] B. Neyenhuis,[1] G. Quéméner,[1] P. S. Julienne,[2] J. L. Bohn,[1] D. S. Jin,[1]† J. Ye[1]†

How does a chemical reaction proceed at ultralow temperatures? Can simple quantum mechanical rules such as quantum statistics, single partial-wave scattering, and quantum threshold laws provide a clear understanding of the molecular reactivity under a vanishing collision energy? Starting with an optically trapped near–quantum-degenerate gas of polar $^{40}K^{87}Rb$ molecules prepared in their absolute ground state, we report experimental evidence for exothermic atom-exchange chemical reactions. When these fermionic molecules were prepared in a single quantum state at a temperature of a few hundred nanokelvin, we observed p-wave–dominated quantum threshold collisions arising from tunneling through an angular momentum barrier followed by a short-range chemical reaction with a probability near unity. When these molecules were prepared in two different internal states or when molecules and atoms were brought together, the reaction rates were enhanced by a factor of 10 to 100 as a result of s-wave scattering, which does not have a centrifugal barrier. The measured rates agree with predicted universal loss rates related to the two-body van der Waals length.

Scientific interest in precisely understanding the fundamental aspects of chemical reactions and controlling their dynamic processes has stimulated pioneering work on molecular beams to study state-to-state reactions using molecular alignment, velocity selections, and angle-resolved measurement (*1*–*5*). However, substantial motional energies remained in earlier work, and thermal statistical averages were a necessary ingredient. By preparing a molecular ensemble's translational degrees of freedom in the quantum regime, we expect to develop fundamental insights into how chemical reaction processes may be precisely guided by quantum mechanics. Reaction dynamics at vanishingly low energies remain a fascinating and yet unexplored scientific realm (*6*). Under unprecedented energy resolution, each step of a complex reaction may be analyzed on the basis of single quantum states and single reaction channels. For example, we can study how reactivity is dictated by the quantum statistics of the molecule as a whole.

That chemical reactions could occur at ultralow temperatures seems at first glance counterintuitive. However, ultracold collisions, where particles scatter only in the partial wave with lowest angular momentum, are governed by quantum statistics and quantum threshold behaviors described by the Bethe-Wigner laws (*7*–*9*). In this regime, particles are represented by their de Broglie wavelength, which increases with reduced temperature. This wave nature of particles replaces our intuitive and classical picture of collisions. The wave manifestation of tunneling through reaction or angular momentum barriers may play a dominant role in dynamics, and scattering resonances can have dramatic effects on reactions (*10*). In addition, any barrierless chemical reactions will always take place when two reactants are sufficiently close together (*11*). In this case, chemical reaction rates will be determined to a large extent by collisional properties at large intermolecular separations, and thus by how the two partners approach each other. Once their separation reaches a characteristic length scale (~$10a_0$, where $a_0 = 0.53 \times 10^{-10}$ m), a chemical reaction happens with a near unity probability. Therefore, chemical reactions can be surprisingly efficient even at ultracold temperatures. Indeed, this model for barrierless reactions predicts loss rates that are universal in the sense that they do not depend on the details of the short-range interactions, but instead can be estimated using only knowledge of the long-range interactions (*12*).

Like the case of collisions of ultracold atoms, the study of ultracold chemical reactions will play a fundamental role in advancing the field of molecular quantum gases. For example, understanding and manipulating collisions of atoms at ultralow temperatures (<1 μK) has been crucial for the realization of quantum degenerate gases (*13*–*15*), Fermi superfluids that provide opportunities to explore the underlying connection between superconductivity and Bose-Einstein condensation (*16*), neutral atom–based systems for quantum information science (*17*–*19*), and strongly correlated quantum gases (*20*, *21*). Ultracold molecules undergo a more diverse set of collisional processes, with distinct inelastic collision mechanisms arising from chemical reactions, in addition to the traditional state-changing collisions seen with ultracold atoms and highly vibrationally excited molecules (*22*). Furthermore,

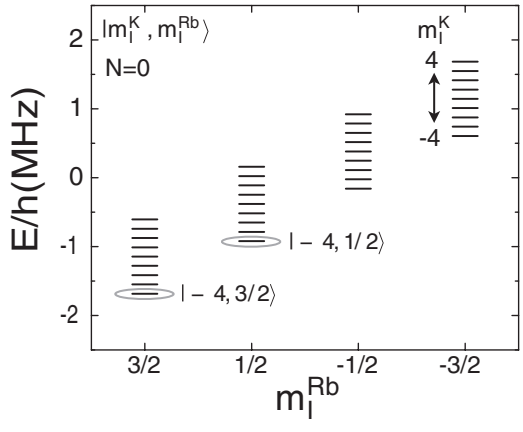

Fig. 1. Hyperfine structure of rovibronic ground-state $^{40}K^{87}Rb$ molecules at 545.9 G. We label the 36 nuclear spin states by their spin projections, m_I^{Rb} and m_I^K. The energy spacing between hyperfine states is ~h × 130 kHz for $|\Delta m_I^K| = 1$ and ~h × 760 kHz for $|\Delta m_I^{Rb}| = 1$. By comparison, at a temperature of 300 nK, the molecules' thermal energy is equivalent to ~h × 6 kHz, which is more than an order of magnitude smaller than the spin flip energy. In our experiments, molecules are prepared in either a single state or in a mixture of $|-4,1/2\rangle$ and the lowest-energy state $|-4,3/2\rangle$ (open ellipses).

[1]JILA, NIST and University of Colorado, Department of Physics, University of Colorado, Boulder, CO 80309, USA. [2]Joint Quantum Institute, NIST and University of Maryland, Gaithersburg, MD 20899, USA.

*These authors contributed equally to this work.
†To whom correspondence should be addressed. E-mail: jin@jilau1.colorado.edu (D.S.J.); ye@jila.colorado.edu (J.Y.)

polar molecules possess anisotropic and long-range dipolar interactions that can be precisely controlled with external electric fields, with rich prospects of collisional resonances (*23*, *24*). Experimental investigation of molecular collisions is essential for such future applications as studying anisotropic and collective behavior in quantum gases (*25*, *26*), modeling new quantum phases and exotic many-body physics (*27*), implementing schemes for quantum information (*28*), and developing tools for precision physical and chemical measurements.

We focus here on the study of ultracold collisions, including chemical reactions, of $^{40}K^{87}Rb$ molecules, which we prepare in their lowest electronic, vibrational, rotational, and hyperfine energy state at a high phase-space density (*29*, *30*). We find clear evidence of the essential role that quantum statistics and quantum threshold laws play in determining the rates of inelastic collisions. Our experimental observations confirm a universal loss mechanism.

Table 1. Summary of the relevant molecular energetics involved in possible chemical reactions. The binding energies are given with respect to the threshold energy for free atoms in the absence of a magnetic field. The $^{87}Rb_2$ and $^{40}K_2$ binding energies include isotope shifts from the data in the respective references. The trimer binding energies are unknown. Calculations of trimer binding energies are needed and will be important for future experiments on any bi-alkali species.

Molecule	$v = 0$ binding energy (D_0)	Reference
$^{87}Rb_2$	3965.8 (±0.4) cm^{-1}	(*45*)
$^{40}K^{87}Rb$	4180.417 cm^{-1}	(*29*)
$^{40}K_2$	4405.389 (±0.004) cm^{-1}	(*46*)
K_2Rb	Unknown	
KRb_2	Unknown	

A prerequisite for exploring ultracold chemical reactions is a gaseous molecular sample that is sufficiently dense, ultracold, and suitable for precise control of specific quantum states (*6*). The starting point for this work is an ultracold trapped gas of fermionic $^{40}K^{87}Rb$ molecules prepared in a single hyperfine level of the rovibronic ground state ($N = 0$, $v = 0$ of $X^1\Sigma^+$) (*29*, *30*). The optical trap depth is ~$k_B \times 10$ μK, where k_B is Boltzmann's constant. The molecules are produced using a single step of two-photon Raman transfer from extremely weakly bound molecules at a magnetic field of ~545.9 G. The coherent transfer is efficient and does not heat the gas, resulting in a gas of rovibronic ground-state molecules with an average number density of 10^{11} to 10^{12} cm^{-3} and a translational temperature of a few hundred nanokelvin. At this ultralow temperature, even the tiny molecular hyperfine-state energy splittings are much larger than the translational energy. Manipulation of the hyperfine states hence becomes extremely important in exploring possible collision channels. In addition, complete control over the internal quantum state of the molecules permits direct observation of the role of quantum statistics in determining the molecular interactions.

A precise measurement of the hyperfine structure and the manipulation of individual hyperfine state populations in the $X^1\Sigma^+$ ground state of $^{40}K^{87}Rb$ were reported in (*30*). The $X^1\Sigma^+$ state has zero total electronic angular momentum, so that the hyperfine structure is basically the Zeeman effect of the nuclear spins $I^K = 4$ and $I^{Rb} = 3/2$ (*12*, *31*) at the applied magnetic field. The hyperfine structure is depicted in Fig. 1, where a total of 36 states are labeled by their projections of the individual nuclear spins, m_I^{Rb} and m_I^K. For the current study, we produce molecules either in a single spin state ($|m_I^K, m_I^{Rb}\rangle$) or in a mixture of two spin states. The hyperfine states used are an excited state $|-4, 1/2\rangle$ and the lowest-energy spin state $|-4, 3/2\rangle$; these are marked by the two ellipses in Fig. 1. The $|-4, 1/2\rangle$ state is populated directly by the two-photon Raman transfer starting from the weakly bound molecules (*29*, *30*). The spin state of these molecules can be further manipulated coherently. For example, the entire $|-4, 1/2\rangle$ population can be transferred into the lowest hyperfine state, $|-4, 3/2\rangle$, using two successive π pulses through a rotationally excited $N = 1$ intermediate level. The $N = 1$ level has strong nuclear electric quadrupole interactions that couple rotations with nuclear spins, enabling nuclear spin flips (*30*, *31*). We can probe molecules in any particular hyperfine state by reversing the entire transfer process and putting the population back into the initial weakly bound state. We then use high–signal-to-noise ratio absorption imaging to measure the molecular gas number and temperature.

The ability to control molecular internal states including the electronic, vibrational, rotational, and nuclear spin degrees of freedom, and in particular the possibility of preparing them in the lowest-energy state, allows us to probe inelastic collisions in a way that limits unwanted loss mechanisms and reduces ambiguities in the identification of possible chemical reaction channels. This is crucial because it is difficult in the ultracold gas experiment to find probes for the direct observation of reaction products. In Table 1, we consider the binding energies for various types of molecules made from different combinations of ^{40}K and ^{87}Rb atoms. These energy estimates allow us to assess whether a specific two-body reaction process is endothermic or exothermic. We note that all results reported here were obtained in the absence of any external electric field, and hence the effective molecular dipole moment in the lab frame is zero.

To probe the quantum nature of ultracold molecular collisions and chemical reactions, we begin by preparing the KRb molecules in a single nuclear spin state of the rovibronic ground state.

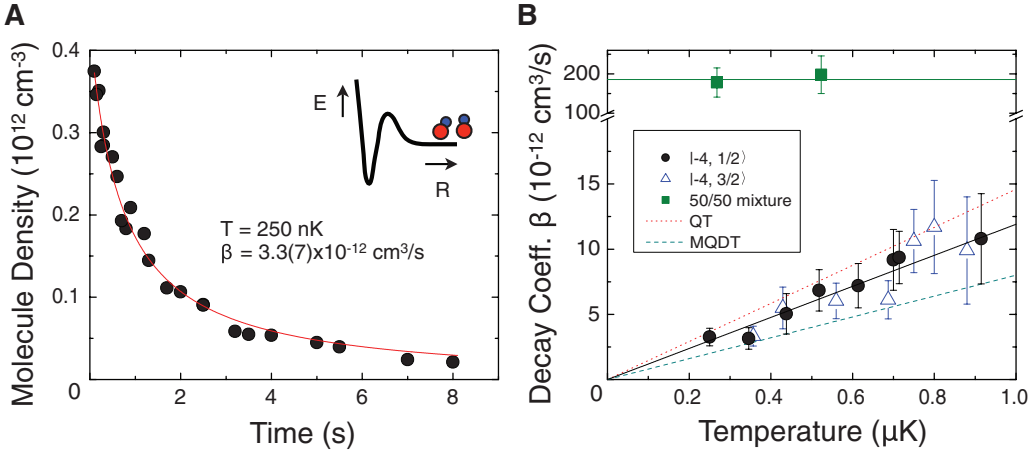

Fig. 2. Inelastic collisions between spin-polarized (indistinguishable) or different spin-state (distinguishable) fermionic molecules in the rovibronic ground state of $^{40}K^{87}Rb$. (**A**) Sample data showing the time dependence of the molecule number density. Here the molecules are prepared in a single hyperfine state, $|-4, 1/2\rangle$, and the molecular density decays slowly with a rate coefficient of 3.3 (±0.7) × 10^{-12} cm^3 s^{-1} at $T = 250$ nK. (**B**) Loss rate coefficient versus temperature. The loss rate increases linearly with temperature for spin-polarized molecules, which collide via p-wave [inset in (A)] at low temperature. Data were taken for molecules prepared in either $|-4, 1/2\rangle$ (solid circles) or the lowest-energy state $|-4, 3/2\rangle$ (open triangles). A linear fit (solid line) to the $|-4, 1/2\rangle$ data yields the temperature-dependent loss rate to be 1.2 (±0.3) × 10^{-5} cm^3 s^{-1} K^{-1}. For the $|-4, 3/2\rangle$ case, where the collisional loss can only be due to chemically reactive scattering, the loss rate is similar. The dotted and dashed lines are theoretical predictions from the QT model and MQDT, respectively. When the molecules are prepared in a mixture of the $|-4, 1/2\rangle$ and $|-4, 3/2\rangle$ states (solid squares), we observe a temperature-independent decay rate that is 10 to 100 times that for the spin-polarized case. The error bars represent 1 SD of the decay rate coefficients arising from fluctuations of the molecular density, temperature, and fitting uncertainty of the two-body loss curves.

All unpaired atoms that remain after the initial stage of the molecular creation process are selectively removed from the optical trap via resonant light scattering (*32*). From an argument based on the energetics summarized in Table 1, the molecule-molecule collisions have a possible exothermic chemical reaction, namely KRb + KRb → K_2 + Rb_2, which releases ~10 cm^{-1} of kinetic energy. The reactions KRb + KRb → K_2Rb + Rb and KRb + KRb → KRb_2 + K could also be exothermic. All of these reactions require breaking and making molecular bonds. If the KRb molecules are prepared in an excited hyperfine state, spin relaxation to a lower hyperfine state provides an additional inelastic scattering mechanism.

The quantum statistics of the molecules plays an essential role in collisions at a temperature of a few hundred nanokelvin, where collisions with large-impact parameters and correspondingly large centrifugal barriers are frozen out and the collisions are typically dominated by a single partial wave with orbital angular momentum quantum number $L = 0$ (s-wave) or $L = 1$ (p-wave). Our KRb molecules are fermions, and therefore the total wave function describing a KRb + KRb collision is antisymmetric with respect to molecular exchange. For spin-polarized molecules all prepared in exactly the same internal quantum state, the p-wave is the lowest-energy symmetry-allowed collision channel. The height of the centrifugal barrier for the $L = 1$ KRb-KRb collisions is $k_B \times 24$ μK (*33*, *34*). This barrier height is more than an order of magnitude larger than k_BT, where T is the translational temperature of the molecular gas. Thus, collisions of spin-polarized molecules are expected to proceed predominantly via tunneling through the p-wave barrier. Note that T is greater than 1.4 times the Fermi temperature. If two molecules make it through the barrier to short range, chemical reactions or hyperfine state-changing collisions can take place, leading to a loss of the entrance channel population. We note that even a single nuclear spin flip corresponds to a released quantity of energy that is above the trap depth, and this would contribute to loss of trapped molecules.

The quantum nature of the collisions can be seen in the temperature dependence of loss rates. The Bethe-Wigner threshold law predicts that the p-wave inelastic/reactive collision rate should be linear in temperature ($\propto T$). To look for this behavior, we first prepared spin-polarized molecules in the single hyperfine state $|-4, 1/2\rangle$ for various values of T ranging from 200 to 900 nK (*35*). The temperature is measured from the expansion energy of the molecular gas after releasing it from the optical trap. For each initial temperature, we observed the time-dependent molecular loss (*36*) and extracted a two-body loss rate β (which is twice the collisional event rate) by fitting the measured decay of the molecular gas density n versus time t (Fig. 2A) to

$$\frac{dn}{dt} = -\beta n^2 - \alpha n \qquad (1)$$

Here, the first term on the right accounts for number loss and the measured β can be compared to theoretical predictions. The second term accounts for density change due to heating of the trapped gas during the measurement. Within a single measurement, we observe an increase in temperature that is at most 30%. In the analysis for each data set, we fit the measured temperature to a linear heating rate and obtain a constant slope c. In Eq. 1, we then use $\alpha = (3/2)[c/(T + ct)]$, where T is the initial temperature. At our lowest temperature of 250 nK, the heating was 7 (±1) nK s^{-1} and $\beta = 3.3\ (\pm 0.7) \times 10^{-12}$ cm^3 s^{-1} (Fig. 2A). The measured dependence of β versus T is summarized in Fig. 2B (solid circles). Here, we fit the data to a power law $\beta(T) \propto T^L$ and find that $L = 1.1$ (±0.2), which agrees with the predicted p-wave threshold law. This result demonstrates that indistinguishable $^{40}K^{87}Rb$ molecules at ultralow temperatures collide via tunneling through a p-wave barrier followed by an inelastic collision in the short range. A linear fit to the data ($L = 1$) yields a slope of the decay rate coefficient of $1.2\ (\pm 0.3) \times 10^{-5}$ cm^3 s^{-1} K^{-1}.

We repeated this measurement for molecules in the lowest hyperfine state $|-4, 3/2\rangle$ (open triangles in Fig. 2B). The data again show $\beta \propto T$ with a slope of $1.1\ (\pm 3) \times 10^{-5}$ cm^3 s^{-1} K^{-1}, similar to that measured for molecules in the $|-4, 1/2\rangle$ state. However, in the case of $|-4, 3/2\rangle$ molecules, hyperfine state-changing collisions are no longer possible and the only possible loss channels are the chemical reactions discussed above. Thus, we find that the rate of chemical reactions is determined by the p-wave angular momentum barrier, and the chemical reaction barrier must be below the collision energy. This suggests that these reactions are barrierless and can thus occur freely at ultralow temperatures. Meanwhile, the fact that the same loss rate is observed for both $|-4, 1/2\rangle$ and $|-4, 3/2\rangle$ state molecules suggests that chemical reactions dominate the loss in these ground-state molecular collisions.

To understand the loss rates, we use two models: a simple quantum threshold model (QT), and a model that uses the formalism of multichannel quantum defect theory (MQDT). In the QT model, the loss rate for collisions with energy equal to or above the height of the p-wave barrier is determined by the Langevin capture rate (*37*), which assumes that the probability for chemical reactions and/or hyperfine state-changing collisions is unity. For all collision energies below the height of the p-wave barrier, we assume in this model that the loss follows the Bethe-Wigner threshold laws (*7*, *8*). Using this assumption, we obtain a simple analytical expression for the p-wave loss rate coefficient of two indistinguishable molecules, which scales linearly with T (*38*):

$$\beta = \frac{\pi}{4}\left(\frac{3^{17}\mu^3 C_6^3}{\hbar^{10}}\right)^{1/4} k_B T \qquad (2)$$

where μ is the reduced mass and $\hbar$ is Planck's constant divided by 2π. Using a van der Waals dispersion coefficient of $C_6 = 16130$ a.u. for KRb-KRb with an uncertainty of ±10% (*33*, *34*), the slope of the rate coefficient is predicted to be $1.5\ (\pm 0.1) \times 10^{-5}$ cm^3 s^{-1} K^{-1}, which agrees well with the experimental measurement.

In the second model, the loss rate coefficient is found directly by calculating the

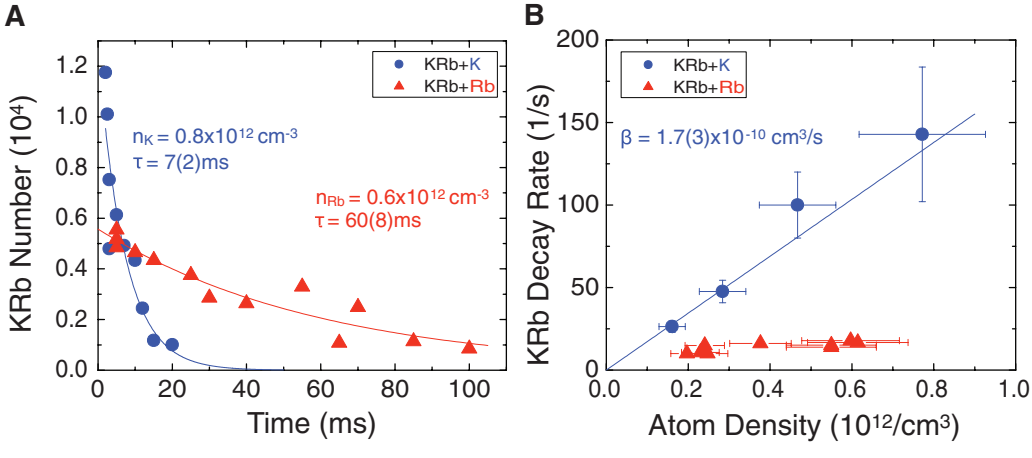

Fig. 3. Collisions of atoms and molecules in their lowest-energy internal states. (**A**) Sample decay curves for the molecular number when subject to collisions with K atoms (circles) and with Rb atoms (triangles). The atom numbers are 5 to 15 times the molecule numbers. The reduced initial molecule number for KRb + Rb is due to the collisional quenching of the initial weakly bound KRb molecules with Rb (*42*) before the two-photon Raman process that transfers the molecules down to the rovibronic ground state. (**B**) Dependence of molecule loss rate on atomic gas density. We observed strong molecule loss with $\beta = 1.7\ (\pm 0.3) \times 10^{-10}$ cm^3 s^{-1} for KRb + K collisions and suppressed loss of KRb for KRb + Rb collisions. The error bars are 1 SD of decay rates and atomic densities.

quantum tunneling rate through the p-wave barrier (*39*). This calculation gives $\beta = 0.8\ (\pm 0.1) \times 10^{-5}$ cm^3 s^{-1} K^{-1}, which agrees with the experiment within mutual uncertainties. This β can also be derived analytically from the properties of the long-range potential to give $\beta = (11.48\,\bar{a})^3\,(k_B T/h)$, where $\bar{a} = 0.4778\,(2\mu C_6/\hbar^2)^{1/4} = 6.3$ nm is the characteristic length of the van der Waals potential (*12*). This fully quantum calculation can be put in the same form as the QT model (Eq. 2) and gives a β that is smaller by a factor of 0.528. With these simple theories, the agreement with our molecule-molecule collisional loss measurements suggests that the chemical reaction rates are strongly influenced by the long-range interactions. This observation opens intriguing control possibilities because the long-range interaction can be controlled by selecting quantum states and tuning collision energies via applied electric and magnetic fields.

Reaction rates should be markedly different if molecules are prepared in a mixture of different hyperfine states as s-wave scattering becomes allowed. We measured the inelastic collision rates for rovibronic ground-state molecules that were prepared in a roughly 50-50 incoherent mixture of the two hyperfine spin states $|-4, 3/2\rangle$ and $|-4, 1/2\rangle$. The time-dependent number density of trapped molecules was measured for both spin states. We observed the same loss rate for both states, consistent with loss due to collisions between distinguishable molecules in different spin states. The rate coefficient is determined to be $1.9\ (\pm 0.4) \times 10^{-10}$ cm^3 s^{-1}, independent of temperature (solid squares in Fig. 2B). In comparison to our measurements for p-wave collisions between spin-polarized molecules, the s-wave collision rate between molecules in different hyperfine states is higher by a factor of 10 to 100 for a similar temperature range.

The MQDT model can also be used to estimate collision rates where the dominant collision channel is s-wave. Here, the relevant length scale is determined by the inter-molecular van der Waals potential without any angular momentum barrier (*40*). We assume that when the molecules approach each other within the van der Waals length $\bar{a}$, chemical reactions take place and remove these entrant molecules with a near-unity probability. The universal loss rate coefficient, $\beta = 2(h/\mu)\,\bar{a}$ (*12*), predicts a β value of 0.8×10^{-10} cm^3 s^{-1}, which is a factor of 2 lower than the experimentally observed value. This difference suggests that short-range physics may play some role in the loss dynamics. An enhancement in the rate coefficient (up to the energy-dependent unitarity limit, which is 4×10^{-10} cm^3 s^{-1} for a gas at 400 nK) is possible if there is a partial reflection of the colliding species back into the entrance channel (*39*). The reflected amplitude interferes with the incoming amplitude and can either increase or decrease the rate coefficient from its "universal" value. Additional theory and experiment are needed to explore this possibility.

In addition to molecule-molecule reactions, the relatively long lifetime of a pure gas of spin-polarized molecules in the optical trap (~1 s) affords time to look for chemical reactions between atoms and molecules. The MQDT model described above can also predict the atom-molecule reaction rates determined by the long-range physics for the universal loss mechanism. To prepare the atom-molecule mixture, we control the atom density by selectively removing or heating unpaired atoms after the initial molecule creation (*41*). For these experiments, we typically work with an atom number about 5 to 15 times the molecule number. All atoms and molecules are prepared in their lowest-energy states at 545.9 G. Specifically, K atoms are in their $|F = 9/2, m_F = -9/2\rangle$ state, Rb in $|F = 1, m_F = 1\rangle$, and KRb in $|-4, 3/2\rangle$. Here F is the total atomic spin and m_F is the spin projection. We performed two separate experiments, one with K and KRb and the second with Rb and KRb, at a temperature less than 1 μK. In both cases, the background of atoms in the other, undesired, species was less than 1000, corresponding to a density below 5×10^9 cm^{-3}. Because both the atoms and the molecules are prepared in their lowest-energy states, trap loss due to inelastic spin-changing collisions is not possible. However, from Table 1, we do expect loss from chemical reactions for the exothermic reaction $K + KRb \rightarrow K_2 + Rb$, whereas the endothermic $Rb + KRb \rightarrow Rb_2 + K$ should be forbidden.

For each experiment, we measured the time dependence of the trapped molecule population. Typical molecular loss curves are shown in Fig. 3A. To extract the inelastic collision rate, we assume that the atom number density is constant. (This is approximately true because the number of atoms is much larger than the number of molecules.) The trapped molecule number should then decay as

$$\frac{d}{dt} N_{\mathrm{molecule}} = -\beta \times N_{\mathrm{molecule}} \times n_{\mathrm{atom}} \quad (3)$$

where N_{molecule} is the number of molecules, n_{atom} is the atomic density, and β is the inelastic rate coefficient. We can then extract β via an exponential fit, $\exp(-\beta \times n_{\mathrm{atom}} \times t)$. As can be seen in Fig. 3B, in general we find that the molecules are lost from the trap at a much faster rate when K atoms are present than when a similar density of Rb is present.

To see if the molecule loss arises from atom-molecule collisions, we measure the dependence of the loss rate on the atom gas density. For the case of KRb + K, we observe a clear linear dependence on the atomic density and extract an inelastic collision rate coefficient of $1.7\ (\pm 0.3) \times 10^{-10}$ cm^3 s^{-1}. This rate coefficient (due to chemical reactions) can again be predicted from the van der Waals length characterizing the long-range part of the potential between the collision partners. Using methods similar to those used for KRb + KRb, Kotochigova has calculated C_6 for KRb + K to be 7020 (±700) a.u. (*34*), which gives a predicted reaction rate of 1.1×10^{-10} cm^3 s^{-1}. Again we find that the MQDT value is close but somewhat lower than the measured value; this result further solidifies the importance of long-range quantum scattering in the inelastic process.

In contrast, for KRb + Rb collisions, the density dependence of the loss rate is not obvious (Fig. 3B). Nevertheless, we again fit the dependence as linear and obtain an upper limit for the rate coefficient of $0.13\ (\pm 0.04) \times 10^{-10}$ cm^3 s^{-1}, which is one order of magnitude smaller than what we measure for KRb + K. Our measurement is consistent with the fact that for KRb + Rb, there is no two-body chemical reaction pathway. A possible mechanism for the residual nonzero rate coefficient for KRb + Rb would be collisions of ground-state molecules with undetected molecules in high-lying vibrationally excited states. These contaminant molecules could be produced by inelastic collisions of Rb atoms with our weakly bound KRb molecules (*42*) before the two-photon Raman process that produces ground-state molecules. Another possible loss mechanism is Rb + Rb + KRb three-body inelastic collisions. Further experiments will be needed to check these possibilities. We note that this suppressed loss rate is observed only when both KRb and Rb are prepared in their lowest-energy internal states at 545.9 G. If either the molecules or the atoms are in an excited hyperfine state, then the observed inelastic rate coefficient rises again to the order of 10^{-10} cm^3 s^{-1}. Therefore, for practical reasons, removing Rb atoms is important for creating a long-lived sample of ground-state KRb molecules.

Together the studies presented here show that we have observed barrierless chemical reactions in the short range, with the rates determined by long-range scattering dynamics dictated by quantum statistics, angular momentum barriers, and threshold laws. We see that a change as seemingly insignificant as flipping a single nuclear spin dramatically changes the rate of molecular collisions. A pure gas of spin-polarized KRb molecules is long-lived in an optical trap (surviving for a time on the order of 1 s) whereas a spin mixed KRb sample decays 10 to 100 times as quickly. Our results clearly show that chemical reactions can proceed with high rates in the ultracold regime.

References and Notes

1. R. N. Zare, *Science* **279**, 1875 (1998).
2. L. Schnieder *et al.*, *Science* **269**, 207 (1995).
3. P. Casavecchia, *Rep. Prog. Phys.* **63**, 355 (2000).
4. K. P. Liu, *Annu. Rev. Phys. Chem.* **52**, 139 (2001).
5. L. Che *et al.*, *Science* **317**, 1061 (2007).
6. L. D. Carr, D. DeMille, R. Krems, J. Ye, *N. J. Phys.* **11**, 055049 (2009).
7. H. A. Bethe, *Phys. Rev.* **47**, 747 (1935).
8. E. P. Wigner, *Phys. Rev.* **73**, 1002 (1948).
9. H. R. Sadeghpour *et al.*, *J. Phys. B* **33**, R93 (2000).
10. N. Balakrishnan, A. Dalgarno, *Chem. Phys. Lett.* **341**, 652 (2001).
11. J. M. Hutson, P. Soldán, *Int. Rev. Phys. Chem.* **26**, 1 (2007).
12. P. Julienne, *Faraday Discuss.* **142**, 361 (2009).
13. E. A. Cornell, C. E. Wieman, *Rev. Mod. Phys.* **74**, 875 (2002).
14. W. Ketterle, *Rev. Mod. Phys.* **74**, 1131 (2002).

15. B. DeMarco, D. S. Jin, *Science* **285**, 1703 (1999).
16. C. A. Regal, D. S. Jin, *Adv. At. Mol. Opt. Phys.* **54**, 1 (2006).
17. D. Jaksch, C. Bruder, J. I. Cirac, C. W. Gardiner, P. Zoller, *Phys. Rev. Lett.* **81**, 3108 (1998).
18. A. Gaëtan *et al*., *Nat. Phys.* **5**, 115 (2009).
19. E. Urban *et al*., *Nat. Phys.* **5**, 110 (2009).
20. I. Bloch, J. Dalibard, W. Zwerger, *Rev. Mod. Phys.* **80**, 885 (2008).
21. T. Kinoshita, T. Wenger, D. S. Weiss, *Nature* **440**, 900 (2006).
22. E. R. Hudson, N. B. Gilfoy, S. Kotochigova, J. M. Sage, D. DeMille, *Phys. Rev. Lett.* **100**, 203201 (2008).
23. A. V. Avdeenkov, J. L. Bohn, *Phys. Rev. A* **66**, 052718 (2002).
24. C. Ticknor, J. L. Bohn, *Phys. Rev. A* **72**, 032717 (2005).
25. T. Lahaye, C. Menotti, L. Santos, M. Lewenstein, T. Pfau, *Rep. Prog. Phys.* **72**, 126401 (2009).
26. S. Yi, L. You, *Phys. Rev. A* **61**, 041604 (2000).
27. G. Pupillo, A. Micheli, H. P. Büchler, P. Zoller, in *Cold Molecules: Theory, Experiment, Applications*, R. Krems, W. Stwalley, B. Friedrich, Eds. (CRC Press, Boca Raton, FL, 2009), chap. 12.
28. A. André *et al*., *Nat. Phys.* **2**, 636 (2006).
29. K.-K. Ni *et al*., *Science* **322**, 231 (2008).
30. S. Ospelkaus *et al*., *Phys. Rev. Lett.* **104**, 030402 (2010).
31. J. Aldegunde, B. A. Rivington, P. S. Żuchowski, J. M. Hutson, *Phys. Rev. A* **78**, 033434 (2008).
32. Residual unpaired Rb atoms are removed immediately after creating weakly bound molecules. We use a sequence that includes adiabatic rapid passage using frequency-swept microwaves for transitioning Rb atoms from $|F = 1, m_F = 1\rangle$ to $|2, 2\rangle$ and then a pulse of laser light resonant with the cycling transition from $|2, 2\rangle$ to $|F' = 3, m_F' = 3\rangle$ to heat the atoms out of the trap. The sequence is performed three times within a time span of 1 ms. Unpaired K atoms are removed immediately after the molecules are transferred into the rovibronic ground state. We apply a 0.5-ms pulse of light on the cycling transition $|F = 9/2, m_F = -9/2\rangle$ to $|F' = 11/2, m_F' = -11/2\rangle$. Any trapped atoms left after this removal are below our detection limit, which is about 1000 atoms.
33. The height of the p-wave barrier is determined by the molecule-molecule long-range potential, namely $[\hbar^2 L(L + 1)/2\mu R^2] - (C_6/R^6)$, for $L = 1$ and $C_6 = 16{,}130\ E_h \times a_0^6$ (a.u.), where $E_h = 4.36 \times 10^{-18}$ J and $a_0 = 0.53 \times 10^{-10}$ m.
34. The calculated van der Waals dispersion coefficients, C_6, used here for KRb + KRb, KRb + K, and KRb + Rb potentials were provided to us by S. Kotochigova. This was done using nonrelativistic ab initio calculations of the dynamic polarizability of KRb in the standard formula for the van der Waals coefficient (*43*, *44*), including the contributions from the spectrum of electronically excited states and the ground-state rovibrational levels.
35. We control the molecular gas temperature by varying the initial temperature of our Rb and K atom gases during forced evaporative cooling.
36. Loss due to blackbody radiation driving either vibrational or rotational excitations is negligible, as this is expected to occur on the time scale of 10^5 s.
37. P. Langevin, *Ann. Chim. Phys.* **5**, 245 (1905).
38. G. Quéméner, J. L. Bohn, http://arxiv.org/abs/1001.5062 (2010).
39. Z. Idziaszek, P. S. Julienne, http://arxiv.org/abs/0912.0370 (2009).
40. T. Köhler, K. Góral, P. S. Julienne, *Rev. Mod. Phys.* **78**, 1311 (2006).
41. To remove selective amounts of K, we partially transfer the population of K atoms from $|F = 9/2, m_F = -9/2\rangle$ to $|9/2, -5/2\rangle$ using two successive radio-frequency (rf) pulses. We then clean out K atoms in the $|9/2, -9/2\rangle$ state using resonant light as in (*32*). Once these atoms are heated out of the trap, we again use rf pulses to spin-flip all K $|9/2, -5/2\rangle$ atoms back down to $|9/2, -9/2\rangle$. To selectively vary the density of Rb, we perform a complete spin flip from $|1, 1\rangle$ to $|2, 2\rangle$ and then turn on resonant light for a duration between 1 and 10 μs. The resonant light both removes Rb atoms and heats the remaining gas. After the resonant light pulse, Rb atoms are transfered back to the lowest hyperfine state $|1, 1\rangle$. We then apply an additional resonant light pulse to remove any residual Rb in $|2,2\rangle$, thus ensuring that all Rb atoms are in the $|1,1\rangle$ state.
42. J. J. Zirbel *et al*., *Phys. Rev. Lett.* **100**, 143201 (2008).
43. M. Marinescu, H. R. Sadeghpour, A. Dalgarno, *Phys. Rev. A* **49**, 982 (1994).
44. S. Kotochigova, E. Tiesinga, *Phys. Rev. A* **73**, 041405 (2006).
45. C. Amiot, *J. Chem. Phys.* **93**, 8591 (1990).
46. St. Falke, I. Sherstov, E. Tiemann, Ch. Lisdat, *J. Chem. Phys.* **125**, 224303 (2006).

47. Supported by NIST Innovations in Measurement Science–Ultracold Stable Molecules, NSF Physics Frontier Center at JILA, U.S. Department of Energy, Air Force Office of Scientific Research MURI on Ultracold Molecules, and a NSF graduate fellowship (B.N.) and by Office of Naval Research grant N0001409IP20041 (P.S.J.). We thank S. Kotochigova for providing her calculations of the van der Waals dispersion coefficients that are relevant to our experiments.

2 November 2009; accepted 28 December 2009
10.1126/science.1184121

Low-Frequency Modes of Aqueous Alkali Halide Solutions: Glimpsing the Hydrogen Bonding Vibration

Ismael A. Heisler and Stephen R. Meech*

The solvation of ions in aqueous media is a fundamental process in biology and chemistry. Here, we report direct time-domain observations of the hydrogen bond vibrational mode formed between a halide ion (chloride, bromide, or iodide) and the surrounding water molecules. The frequency of the hydrogen bond mode is sensitive to both the atomic weight and the concentration of the ion. The peak frequencies fall in the 125 to 175 wave-number range, a spectral region accessed through time-domain polarization-resolved coherent Raman scattering using a diffractive optic method. The polarized Raman response observed is discussed in terms of the structure of the anion's solvation shell and modeled through calculations on water chloride clusters.

Aqueous solvation of ions is a central process in many chemical and biological reactions. It plays a critical role in determining acid-base equilibria (*1*), interface structure (*2*), and ion transport in electrolyte solutions (*3*) and across membranes (*4*). Aqueous solutions of alkali halide salts present the archetypal example of solvation and have consequently been studied in great detail through both experiment and simulation (*5*). Important progress in understanding the microscopic structure and dynamics of solvated ions has recently been made through ultrafast vibrational spectroscopy (*6*–*9*) and molecular dynamics simulation (*10*–*14*). Most of these experiments focused on the readily observable infrared (IR)–allowed OD stretch of monodeuterated water (HOD) in aqueous solutions of alkali halides. The vibrational relaxation and molecular orientational relaxation times observed are significantly slower compared with the same measurements for HOD in pure H_2O and become slower still with increasing concentration of the electrolyte (*7*, *9*). Two-dimensional IR spectroscopy on the OD stretch reveals further information on the molecular dynamics, suggesting a hierarchy of relaxation times. The fastest component arises from local fluctuations in the length of the OD···X^- hydrogen bond (H-bond), where X^- is the anion. The intermediate (subpicosecond) and longer (picosecond) relaxation components, which increase with increasing halide ion concentration, reflect the transition from local H-bond fluctuations to global reorganization and the reorganization of H-bond networks, respectively (*9*). From these studies of the OD mode, inferences on the structure and dynamics of the OD···X^- H-bonds are drawn. However, the H-bond mode itself is not well characterized, and a more complete description of it will help to refine the analysis and simulation of aqueous solvation dynamics.

Here, we report direct time-domain experimental observations of the spectra of the OH···X^- hydrogen bond through measurements of the low-frequency isotropic Raman response. To access the low-frequency region of the spectrum, where H-bond modes are expected to appear, we probed in the time domain the decay of polarization induced in the sample by an ultrafast pump pulse (*15*). In a two-beam pump-probe configuration, this experiment measures the transient optical Kerr effect, which, when combined with heterodyne detection and Fourier transform analysis, yields the Raman spectral density with excellent signal-to-noise ratio in the 0- to 500-cm^{-1} region (*16*). In the present experiments, we exploited a four-beam transient grating diffractive optic geometry, described in detail by Goodno *et al*. (*17*). Essentially, pump and probe beams are focused onto a diffractive optic element to

School of Chemistry, University of East Anglia, Norwich NR4 7TJ, UK.

*To whom correspondence should be addressed. E-mail: s.meech@uea.ac.uk